Appl Magn Reson (2009) 36:195–208
DOI 10.1007/s00723-009-0018-2

Applied
Magnetic Resonance

Magnetic Field Effect in the Reaction of Recombination of Nitric Oxide and Superoxide Anion

Tatiana Yu. Karogodina · Svetlana V. Sergeeva · Dmitri V. Stass

Received: 13 October 2008 / Revised: 13 March 2009 / Published online: 17 October 2009

Abstract Using a static magnetic field, we observed an important biological radical, nitric oxide, in solution by a spin-sensitive technique. Decomposition of 3-morpholinosydnonimine (SIN-1) in aqueous solution produces a radical pair consisting of nitric oxide and the superoxide anion which recombine to form peroxynitrite. The creation of this radical pair provides a favorable setting for the observation of magnetic field effects. Magnetic field effect of $(1.8 \pm 0.5)\%$ on the yield of recombination was observed in a relatively high field of 4.7 T over the sampling of 96 samples. The effect is limited by extremely fast relaxation of nitric oxide in liquids due to unquenched orbital angular momentum, and develops in f-pairs via the Δg mechanism. Magnetic field effect due to a radical pair involving nitric oxide in a biological system would require either rather strong magnetic fields in the tesla range or an internal enhancer of magnetic field.

1 Introduction

Magnetic field effects (MFEs) have long been discussed in biological context. Starting from sheer curiosity issues, they have grown into a major concern due to the increasing presence of artificial magnetic and electromagnetic fields in the environment and their possible health implications [1]. A huge body of data, from epidemiologic surveys to deliberate experiments on humans through to cell cultures

T. Yu. Karogodina · D. V. Stass (✉)
Institute of Chemical Kinetics and Combustion SB RAS, 630090 Novosibirsk, Russia
e-mail: stass@ns.kinetics.nsc.ru

S. V. Sergeeva
Institute of Cytology and Genetics SB RAS, 630090 Novosibirsk, Russia

D. V. Stass
Novosibirsk State University, 630090 Novosibirsk, Russia

and model biochemical systems in vitro, has been accumulated and analyzed but complete understanding of the biological MFE has not yet emerged [2]. The interpretation of MFE in real biological systems, provided they had been reliably established, is very much complicated by the complexity of the objects and the huge distance between the macroscopically measured parameters and the underlying molecular processes that are believed to mediate the MFE [3]. On the other hand, extensive reproducible and well-understood MFEs have been reported on model chemical systems [4] but they usually do not offer a direct link to biological systems. To bridge this gap, an adequate model system, simple enough to allow borrowing of ideas from chemical studies but still rich enough to be relevant for biology, is required. Several such systems have been recently suggested, including cobalamin-dependent enzymatic systems [5, 6], horseradish peroxidase enzymatic systems [7–10], singlet oxygen production in a photosynthetic system [11], enzymatic phosphorylation [12, 13], and cryptochrome photoreception-based magnetic compass [14–18].

Of the several mechanisms invoked to explain biologically relevant MFE, the most consistent so far seems to be the radical pair mechanism [19], implying the presence of a spin-correlated radical pair along the reaction path and its spin-selective recombination [20]. In such systems, a magnetic field can change the rate of radical pair recombination by changing the ratio of the reactive singlet versus non-reactive triplet channels. The radical pair mechanism was established and verified on model chemical systems and was shown to operate in the five systems cited above. To produce an MFE via the radical pair mechanism, two radicals must be present in the system and recombine into an observable product. The radicals can be either directly formed as a spin-correlated pair from the same precursor molecule, or can meet at random in the bulk; provided that their recombination is spin-selective, MFE can be expected in both cases. The majority of the reported MFEs were observed on the initially correlated pairs that provide more favorable conditions with the effects of the order of several percent [4, 20], but MFEs from randomly encountering pairs, where the correlation is induced at contact and the effect is usually smaller, have also been reported [21, 22]. Possible effect of magnetic field on radical pairs is also called upon to explain MFE in complex biological systems involving radicals, but often the radical pair mechanism is invoked solely based on the presence of radicals, such as nitric oxide, in the system. Although not impossible, this logic has three serious problems: the complexity of the real biological systems, the lack of correlation in thus reacting radicals, and their difference from "normal" partners of the spin-correlated pairs. To address all these issues, we have created a model system based on the recombination of nitric oxide (NO) and superoxide radical (O_2^-).

Nitric oxide and superoxide can be generated simultaneously by the decomposition of 3-morpholinosydnonimine (SIN-1) [23], yielding the two radicals that further recombine with a nearly diffusion-controlled rate constant [24] to form peroxynitrite ($ONOO^-$) [25, 26]. In oxygenated aqueous solutions the molecule of SIN-1 transforms into the intermediate product SIN-1A, transfers an electron to a dioxygen molecule to form O_2^-, and then decomposes producing NO and a non-radical end product SIN-1C [27]. The two radicals are formed in rapid succession,

but the delay between their formation is not yet known [27], and depending on it the pair could be formed either in-cage or at random encounter. However, this difference is of secondary importance here, as in both cases the correlated pair will be formed in a triplet state: either directly from the singlet molecule of SIN-1 and the triplet molecule of dioxygen for in-cage generation, or due to spin-selective recombination inducing predominantly triplet spin state of the pairs surviving the first contact in the free pairs. Thus, a simple chemical system exists that can be used to study MFE on a pair of biologically relevant radicals. Here we report the effect of the static external magnetic field on the yield of recombination of nitric oxide and superoxide anion generated upon decomposition of SIN-1 in aqueous solution, monitored by the amount of produced peroxynitrite, and discuss its possible implications for magnetobiology.

2 Experimental

All experiments were conducted at room temperature in aqueous phosphate buffer (KH_2PO_4/K_2HPO_4, 99.0%, Fluka, pH 7.6) [28] with added complexone (50 mM diethylene triamine pentaacetic acid, DTPA) [29] to eliminate the traces of transition metal ions. Peroxynitrite was determined using dihydrorhodamine-123 (DHR-123) [30]. DHR-123 practically does not react with nitric oxide, superoxide anion, and hydrogen peroxide [31–33], while peroxynitrite oxidizes DHR-123 into a persistent colored rhodamine-123 (RH-123) having a characteristic absorption band with $\lambda_{max} = 500$ nm, $\varepsilon = 74500\ M^{-1}\ cm^{-1}$. The yield of RH-123 in this process is 40–44% by the amount of peroxynitrite and strongly depends on such experimental conditions as pH, sample composition, temperature, etc. [24]. Furthermore, solutions of SIN-1 [34] and DHR-123 [33] are sensitive to light and air. Because of these complications and uncertainties only the relative experiments, i.e., comparing exposed and control but otherwise identical samples, were reliable.

The samples were prepared by adding SIN-1 (3-morpholinosydnonimine hydrochloride, Molecular Probes, ICN Biomedicals, Inc) and DHR-123 (dihydrorhodamine-123, SIGMA, $\geq$95%) to the buffer. Superoxide dismutase (SOD, lyophilized, $\sim$98% protein, CuZn, from bovine erythrocytes, balanced potassium phosphate buffer, SIGMA, $M = 32500\ g\ mol^{-1}$, 4470 units mg^{-1}) was used to break the pair in the preliminary experiments [35]. For each experiment a common incubation mixture was always prepared and then divided into samples of 400 µl each. Static magnets with induction of 50 mT (ceramic) and 4.7 T (superconducting) were employed, and the samples were protected from light. The amounts of accumulated RH-123 in the samples were determined from their optical absorption spectra taken in a 1-mm cuvette on a Shimadzu UV-2401 spectrometer; the absolute accuracy of measuring optical density in a single experiment was verified to be $\pm$0.001, consistent with the technical specifications on the reproducibility of the spectrometer.

For each experiment MFE was determined as the relative difference of the average optical densities at 500 nm for a group of samples held in the magnetic field and a group of control samples: $(D_m - D_c)/D_c \times 100\%$. To discard doubtful

results, we used the Q-criterion for confidence probability $P = 0.90$. The errors in MFE for individual experiments were calculated using the law of error propagation. Evaluation of the average MFE and its confidence interval over multiple experiments are discussed later in Sect. 4.

3 Choice of Magnetic Field Strength for Experiments

To produce observable effects, the applied magnetic field must induce transitions between singlet and triplet spin states of the pair while it exists in its correlated state [36]. There are two relevant mechanisms for moving one electron spin with respect to another and thus changing the collective spin state of the pair. The hyperfine mechanism involves interaction of the spin with magnetic nuclei, e.g., protons or nitrogens, which effectively creates additional magnetic field for each electron spin. If these fields are different, the spins precess at different frequencies and/or about different directions and thus change their relative orientation. In the Δg mechanism, the different sensitivities of the two spins to magnetic field (their g values) induce singlet–triplet transitions at a frequency $\omega = (g_1 - g_2)\beta_e B_0/\hbar = \Delta g \beta_e B_0/\hbar$, where g_1 and g_2 are the two g values, β_e is Bohr magneton, and B_0 is the induction of the applied magnetic field. The higher the field, the faster the interconversion, while in the hyperfine mechanism raising the applied field beyond the field of the nuclei saturates the effect at a frequency $\omega \sim g\beta_e A/\hbar$, where A is the hyperfine coupling constant. The time τ available for spin transitions is limited either by the lifetime of the solvent cage, while the radicals remain partially correlated and close to each other after the first encounter, or by the spin relaxation time, whichever is smaller. To observe an effect, the product $\omega\tau$ should at least approach 1.

Nitric oxide in the gas phase has a rather strong intrinsic spin–orbit coupling due to an electronically degenerate $^2\Pi$ ground state [37] (spin–orbit coupling constant $\Lambda = 123\ \mathrm{cm}^{-1}$), which can substantially alter the behavior of the spins in the radical pair "nitric oxide/superoxide anion" in liquids because of potentially extremely fast spin relaxation processes [38]. The ^{14}N hyperfine coupling constant ($A/g\beta_n$) and the g-value for the magnetic $^2\Pi_{3/2}$ substate in the gas phase are about 1 mT and 0.78, respectively [39, 40]. On the other hand, it is possible that due to the interaction with the medium the electronic degeneracy of the semioccupied molecular orbital in the radical is lifted to such a degree that the orbital momentum of the molecule is effectively quenched, thus quenching the spin–orbit interaction. This is, for example, the case for superoxide anion in solid alkali metal superoxides and in the more bulky organic superoxides [41], as well as for hydroxyl radicals in irradiated ice [42]. Superoxide anion, also possessing $^2\Pi$ electronic ground state in the gas phase, produces g-values of 2.0–2.1, indicative of the quenched momentum, in frozen aqueous or acetonitrile solutions [43], and has no hyperfine interactions since the dominant naturally abundant isotope (^{16}O) is nonmagnetic. Nitric oxide was reported to magnetically behave like free gas in frozen clathrates [44]. The situation with the two radicals in our system is not known, and two limiting cases of the effective strength of the spin–orbit coupling in the molecule of nitric oxide can be considered:

1. Interactions with the medium do not quench the electronic degeneracy, and the spin–orbit coupling constant for the molecule of NO is as large as it is in the gas phase (about 120 T in magnetic field units, approaching thermal energy). This means that the spin of the unpaired electron is rigidly coupled to the orbital angular momentum of the molecule directed along the molecular axis, and closely follows it. Collisions with molecules of the medium tumble the molecular axis and thus the spin, which results in very fast paramagnetic relaxation. In this case, to observe any MFE the frequency of singlet–triplet transitions should approach at least the frequency of molecular collisions in liquids ($\sim 10^{12}$–10^{13} s^{-1}), which is rather high. On the other hand, the strong spin–orbit coupling also results in substantially shifted g-values, so that the difference in the g-values of the two partners of the pair is large ($\Delta g \sim 1$). Thus, the required rate of singlet–triplet transitions can be achieved via the Δg mechanism with magnetic fields of 1–10 T. MFEs due to the Δg mechanism in the case of the strong spin–orbit coupling have indeed been reported [45].
2. Interactions with the medium completely quench the orbital angular momentum of the NO molecule. The electron spin becomes essentially independent of its motion, as in the case of "normal" radicals, the relaxation times become rather long (microseconds), and the g-values of the pair partners become essentially equal ($\Delta g \sim 10^{-3}$). The required singlet–triplet transitions can be driven by the hyperfine mechanism in relatively weak fields, provided the frequency of singlet–triplet transitions is of the order of $g\beta A/\hbar$, or about 10^9 s^{-1} for the NO/O_2^- pair. In this case, the hyperfine mechanism can provide efficient singlet–triplet transitions in relatively weak magnetic fields of several tens of millitesla, as has been reported many times for conventional radical pairs [4].

Thus, very different situations are possible depending on the (unknown) degree of orbital angular momentum quenching and hence the strength of the spin–orbit coupling in the molecules of nitric oxide and superoxide anion in liquid. We employed static magnets with induction of 50 mT (ceramic, sufficient to saturate the hyperfine mechanism) and 4.7 T (superconducting magnet of a 200 MHz nuclear magnetic resonance (NMR) spectrometer, sufficient to drive the Δg mechanism), starting with the technically simpler lower magnetic field.

4 Results

4.1 Detection Protocol

Peroxynitrite formed in the decomposition of SIN-1 can be determined by spin-trapping techniques combined with electron spin resonance (ESR) using 1-hydroxy-3-carboxy-2,2,5,5-tetramethyl pyrrolidine (CPH) as the trap [46], or by oxidation of DHR-123 monitored by optical absorption [30]. Spin trapping was initially attempted (data not shown here) but turned out to be unsuitable to detect MFE in this system. It was found that to avoid errors due to unequal timing of measuring the control and exposed samples in which the reaction is initiated simultaneously, the

decomposition had to be completed by the moment of measurement. Therefore, the reaction must be limited by SIN-1 rather than the dissolved O_2 (concentration about 260 μM) to ensure complete decomposition of SIN-1 by the moment of measurement. This safeguards against restarting the decomposition of the remaining SIN-1 upon stirring and reoxygenating the sample during measurements. This, in turn, meant low concentrations of SIN-1 (normally 50 μM), leading to low amounts of peroxynitrite and thus low amounts of the oxidized spin trap, which produced very noisy ESR spectra and unacceptable measurement errors. Optical measurements with DHR-123 turned out to be much more reliable and were used for all experiments discussed here. The reported efficiency of DHR-123 oxidation by peroxynitrite is 40–44% with respect to the amount of available peroxynitrite [24], so the concentration of DHR-123 was set at 50 μM (twofold excess). Figure 1a shows typical absorption spectra—kinetics of RH-123 buildup in the sample containing 50 μM of SIN-1 and 50 μM of DHR-123 followed for 6 h. The expected amount of RH-123 (about 25 μM) was accumulated. All further results were obtained in the same conditions and will be presented in the units of optical density

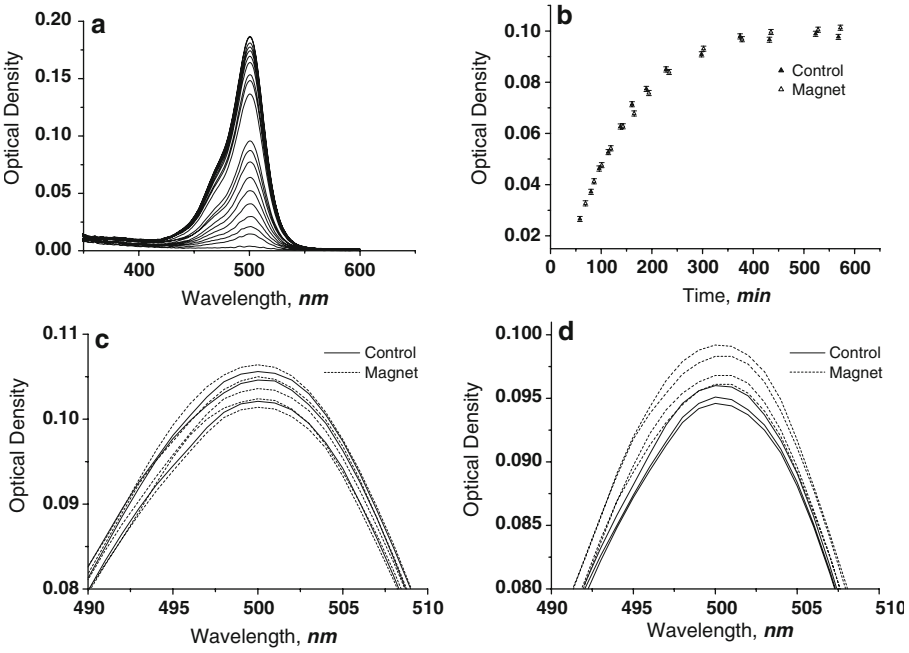

Fig. 1 **a** Development of optical absorption from a solution containing 50 μM of SIN-1 and 50 μM of DHR-123 (time span of 6 h; room temperature, spectra taken in a 1-mm cuvette). **b** Accumulation of RH-123 in samples, containing 50 μM of SIN-1, 50 μM of DHR-123, and 20 units ml^{-1} of SOD, in magnetic field of 50 mT (*open triangles*), and in otherwise identical control samples (*filled triangles*). *Bars* show the error of single measurement. **c** Absorption bands from samples, containing 50 μM of SIN-1, 50 μM of DHR-123, and 20 units ml^{-1} of SOD, exposed for 12 h to magnetic field of 50 mT (*dashed lines*), and from otherwise identical control samples (*solid lines*). **d** Absorption bands from samples, containing 50 μM of SIN-1, 50 μM of DHR-123, and 20 units ml^{-1} of SOD, exposed for 12 h to magnetic field of 4.7 T (*dashed lines*), and from otherwise identical control samples (*solid lines*)

rather than the amount of RH-123. As a scavenger for superoxide anion, 20 units ml^{-1} of SOD was sufficient to halve the yield of the product and this was used in the preliminary experiments.

Systems based on the solutions of SIN-1 are usually employed as donors of nitric oxide and in certain cases peroxynitrite. As the goal in this case is a steady generation of the species, the beginning of the linear portion of the decomposition kinetics of SIN-1 is commonly used. At these relatively short times, side reactions, as well as the actual conditions of conducting the decomposition, are relatively non-critical. However, in this study, we had to look for the MFE by monitoring the total accumulated reaction product over rather long times. A series of separate experiments (data not shown here) was conducted to check how critical were ambient light conditions [33, 34] and extraneous oxidation of DHR-123 [32] in our experimental settings, with the result that protecting the samples from light during the reaction was sufficient to rule out the side processes.

4.2 MFE

Figure 1b shows the curves of RH-123 accumulation in the samples exposed to magnetic field of 50 mT and in the control samples held in a mu-metal box to shield them from stray magnetic fields. A common incubation mixture containing 50 μM of SIN-1, 50 μM of DHR-123 and 20 units ml^{-1} of SOD was prepared and divided into two groups (12 + 12) of samples. As the reaction progressed, the samples were taken out one by one, measured, and discarded. It can be seen that the two curves coincide within experimental accuracy, as the sought effects were expected to be small in first place, and that characteristic reaction time is about 10 h. The method of building the complete kinetic curves does not allow collecting the statistics required for their detection with realistic numbers of samples. More adequate in these circumstances is looking for MFE on the amount of the final reaction product, i.e., in one point with respect to time, but collecting the statistics. Further experiments showed that 12 h was sufficient for complete decomposition of SIN-1 and the completion of the reaction of peroxynitrite with DHR-123 in the samples of defined composition kept at room temperature. In all subsequent experiments both magnetic field and control samples were exposed for not less than 12 h.

In a typical "end-of-process" experiment at 50 mT, a common incubation mixture containing 50 μM of SIN-1, 50 μM of DHR-123, and 20 units ml^{-1} of SOD was divided into two groups of samples which were protected from the light by wrapping the samples in foil. The first group of samples was placed in the magnetic field, and the samples of the second group were placed in a mu-metal box. Sample preparation and placement was completed in 4–6 min, of which the critical stage of wrapping took no longer than 2 min. After the completion of the reaction (12–13 h), optical absorption spectra were taken for all samples in random order and the MFE was evaluated. Figure 1c shows the spectra from one such experimental run. This procedure was repeated three times, but the observed effect was too small (less than 1% over 28 samples) to be measured accurately and reproducibly. Before collecting more significant statistics, a higher MFE in a single experiment was required. This was achieved by additionally engaging the Δg mechanism by moving

to higher magnetic fields. Consequently, further experiments were performed in a magnetic field of 4.7 T.

Incubation mixtures containing 50 μM of SIN-1, 50 μM of DHR-123 and 0, 20 or 400 units ml^{-1} of SOD were prepared and divided into two groups of samples. The samples of the first group were placed in the bore of the 4.7 T magnet in the working region, and the samples of the control group were put in the top region of the bore with the measured magnetic field induction about 1 mT, which had been found to be too low to cause any observable effects. The reason for putting the control samples in the bore as well was the necessity to ensure that the temperature difference between the two groups of samples was as small as possible. The measurement of the temperature profile in the bore demonstrated that the temperature difference between the two groups did not exceed 0.5°C. Figure 1d shows the result of one experimental run in the field of 4.7 T at 20 units ml^{-1} of SOD, with evaluated MFE of (2 ± 2)%. Eight such experiments were performed with varying concentrations of SOD; the calculated MFEs for the experiments were as follows: for SOD activity 20 units ml^{-1} $\varphi_1 = (2 \pm 2)\%$ (or $(2.5 \pm 1.7)\%$, keeping the next decimal place), $\varphi_2 = (1 \pm 2)\%/(1.1 \pm 2.4)\%$, $\varphi_3 = (1 \pm 2)\%/(1.2 \pm 2.5)\%$; for SOD activity 400 units ml^{-1} $\varphi_4 = (2 \pm 3)\%/(1.5 \pm 3.2)\%$, $\varphi_5 = (4 \pm 2)\%/(3.6 \pm 2.0)\%$, $\varphi_6 = (1 \pm 2)\%/(0.9 \pm 2.1)\%$; without SOD $\varphi_7 = (1 \pm 3)\%/(1.4 \pm 3.2)\%$, $\varphi_8 = (2 \pm 1)\%/(1.6 \pm 1.4)\%$.

The observed independence of MFE of the concentration of SOD is consistent with the limiting case of having a very short relaxation time for the radical pair. MFE develops only in the correlated pair, and under these condition, the pair loses correlation already in the cage, where the scavenger cannot yet reach it at any sensible concentration. The observed reaction indeed proceeds in the cage formed when the two radicals first encounter, but it is field-dependent only for very brief flashes after each reencounter, and then the Δg mechanism is at work. Since the presence of SOD in the sample suppresses the formation of peroxynitrite, it reduces the measured optical density. Furthermore, it chemically complicates the system; in particular, OH radicals are produced via dismutation of O_2^- that can also oxidize DHR-123 [32]. To avoid these now unnecessary complications, the final accumulation of statistics was performed on samples without SOD. A total of eight independent experiments of (6 + 6) samples containing 50 μM of SIN-1 and 50 μM of DHR-123 were performed in the field of 4.7 T, with one representative run of this batch shown in Fig. 2a. The dashed traces were taken from the exposed samples, the solid traces from the control ones, and bold curves of each type show the average traces over each group of samples with the corresponding error bars. All experiments showed a systematic increase in the yield of the product with an applied magnetic field.

In all experiments there was a systematic temperature difference of about 0.5°C between the exposed (warmer) and control samples, and the efficiency of DHR-123 oxidation by peroxynitrite is known to depend on temperature [24]. To check whether this could have caused the observed systematic differences in the yield of RH-123, we used the bore of a similar magnet that was idling without the field. Measurements showed that the bore provided a very stable temperature environment with the difference between the temperatures of its two ends of just the sought

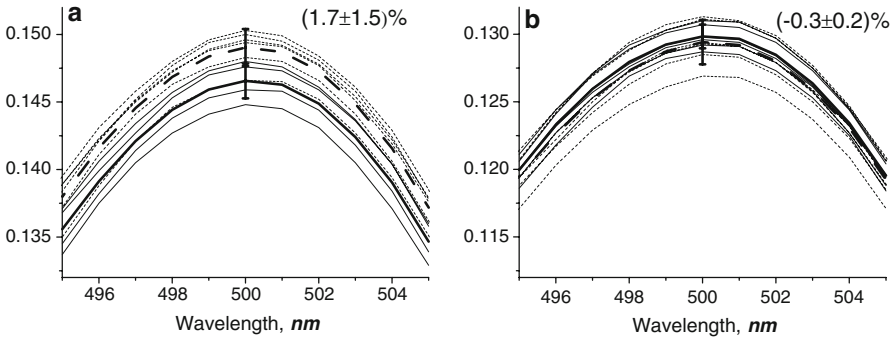

Fig. 2 **a** Absorption bands from six samples, containing 50 μM of SIN-1 and 50 μM of DHR-123, exposed for 12 h to magnetic field of 4.7 T (*dashed lines*), and from six otherwise identical control samples (*solid lines*). *Bold dashed* and *solid lines* show averaged bands from each group of samples with error bars, the number in the *upper right corner* shows evaluated magnetic field effect with RMS error, one of eight individual experimental runs. **b** One of four independent temperature control experiments in the same format, *dashed lines* refer to warmer samples

0.5°C. An incubation mixture containing 50 μM of SIN-1 and 50 μM of DHR-123 was prepared and divided into two groups of six samples, shielded from light, that were put in the bore of the magnet. After the completion of the reaction, optical absorption spectra were measured for all samples, and the effect was calculated as the difference between the average optical densities at 500 nm of the samples from the regions of the higher and lower temperatures, referred to the average optical density of the colder samples: $\varphi = (D_+ - D_-)/D_- \times 100\%$. The experiment was repeated four times, with one representative run shown in Fig. 2b in the same format; the traces for warmer samples are shown in dashed lines.

4.3 Statistical Evaluation of Experimental Data

To evaluate MFE in the field of 4.7 T, eight independent experimental series were obtained. Each series included optical density at 500 nm from six samples exposed to magnetic field and six otherwise identical control samples. Average optical densities at 500 nm and standard deviations were calculated for the exposed (D_m) and control (D_c) groups of samples in each experiment; MFE was calculated as $(D_m - D_c)/D_c \times 100\%$, and its standard deviation was calculated using the law of error propagation. Four independent experimental series were obtained and evaluated without applying the magnetic field, but keeping the temperature difference of 0.4–0.5°C similar to the MFE case. Thus calculated effects are shown next to both panels in Fig. 2 as the mean value with root-mean-square (RMS) error, Fig. 3 shows the results of individual MFE and control experiments as diagrams with mean values and RMS error. To discard doubtful results, each experimental series was tested using the Q-criterion for the confidence probability $P = 0.90$ prior to averaging. As the differences between samples in each experiment were rather tight in absolute magnitude, a broad confidence interval with the probability of 0.90 was adopted to avoid odd discarding.

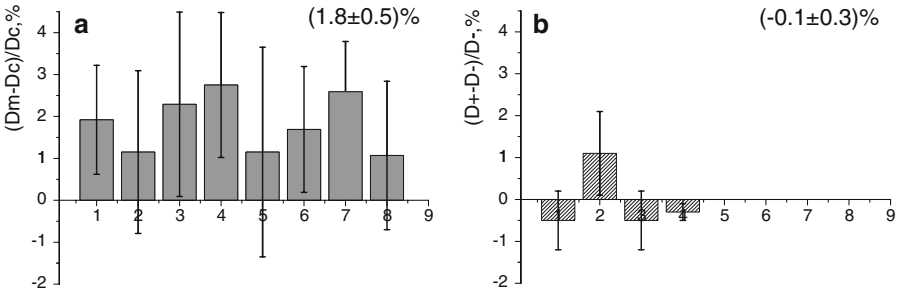

Fig. 3 Evaluated MFEs with standard deviations for each of eight individual experiments with applied magnetic field (**a**) and four temperature controls (**b**). Experiment 6 and Control 4 were shown in Fig. 2. The numbers in the *upper right* corner show average magnetic field and temperature control effect over multiple experiments

Before attempting further statistical evaluation, it was necessary to determine whether the differences between the eight individual MFEs (and four individual controls) should be interpreted as random and whether they provide an estimate of the standard deviation of a single population. This was done in two steps [47]: (1) comparison of RMS errors (using the Bartlett criterion with the one-sided confidence probability $P = 0.95$), and (2) comparison of sample mean values (comparison of differences between sample mean values with differences inside each sample using the Fisher criterion with the one-sided confidence probability $P = 0.95$). The differences between different statistical samples (between different experimental runs) were found to be too significant to allow unifying all measurements of each type (e.g., all 8×6 samples in the field of 4.7 T or all 4×6 warm control samples) into a single population; thus two-step averaging was employed, first calculating MFE for each experiment and then averaging them into the final value. The confidence interval was calculated for the probability $P = 0.95$ as $\pm St/\sqrt{n}$, where n is the total number of measurements across all samples. MFE in the field of 4.7 T over eight experiments with 6 plus 6 samples each amounted to $\varphi = (1.8 \pm 0.5)\%$, and the effect in the four control experiments amounted to $\varphi = (-0.1 \pm 0.3)\%$. The observed changes in the amount of measured RH-123 are indeed connected with the applied magnetic field.

5 Discussion

Thus, in the relatively high field of 4.7 T an MFE of $(1.8 \pm 0.5)\%$ was observed. The obtained experimental results can be explained with the following model:

In the decomposition of SIN-1 in aqueous solution at room temperature, peroxynitrite is formed upon the recombination of free pairs of NO and O_2^- radicals. Both nitric oxide and superoxide radicals have rather strong spin–orbit coupling in the gas phase that effectively aligns the spins along the molecular axes, and at least for one of the radicals, nitric oxide, this coupling is not quenched by the interaction with the medium in the aqueous phosphate buffer solution. Thus, the pair

of NO and O_2^- radicals has spin relaxation times of the order of molecular tumbling in solution, about 10^{-12}–10^{-11} s (1–10 characteristic collision times in solution), and a substantial difference in the *g*-values of the pair partners of the order of unity. A static external magnetic field can then affect pair recombination via the Δg-mechanism for the field strength 1–10 T, which accounts for the absence of a statistically reliable effect in a relatively weak field of 50 mT and for the observed effect in a field of 4.7 T. MFE is developed in short ($\sim 10^{-11}$ s) flashes after each reencounter, during which the pairs remain correlated.

Although small, the reported MFE is measured directly as opposed to MFE evaluated as changes of parameters extracted from modeling, and the obtained magnitudes are rather reliable. Furthermore, it follows that the actual mechanism of generating NO becomes unimportant due to the intrinsic properties of this radical, since spin relaxation becomes the dominant factor, and the formation of the pair as a free pair is not a limitation. Although we have used a simple chemical system to generate the two radicals, the inferred conclusions can be generalized to other systems containing free nitric oxide, including naturally occurring enzymatic nitric oxide synthases.

As mentioned in Sect. 1, attempts are sometimes made to explain the observed macroscopic MFE for moderate magnetic field strength on complex biological systems by the action of magnetic field on the radical pairs, including the NO/O_2^- pair. Our data suggest that any direct effect on the radicals of this type would require rather strong fields, at least in the tesla range. However, such effects may well be possible if a biological system provides a means of enhancing either the external field or its effect. When transferring the results from in vitro experiments with NO into a biological context it should be taken into account that NO is a retrograde mediator initiating a cascade of processes in organisms [48], and thus even small changes in its concentrations can have far-reaching cumulative effects. Regarding the internal enhancement of the applied magnetic field, environments where biogenic iron is accumulated are not uncommon in biology, and a situation reminiscent of ferrofluids [49, 50] with a stable dispersion of paramagnetic particles can occur. An example of the enhancer effect is a 30-fold activity increase of horseradish peroxidase that was recently reported in a weak magnetic field in the presence of magnetite particles [51]. Certain pathologies, in particular thalassemia [52, 53] and age-related neurodegenerative diseases [54, 55], are accompanied by accumulation of biogenic iron. Substantia nigra neuromelanin [56], an age-related pigment that can bind thousands of iron atoms into a chemically inert paramagnetic granule and whose function is yet unclear, can also be a plausible candidate for such a biogenic field enhancer. It may also become possible to reconcile two competing theories of biological MFE, due to radical pairs and due to biogenic magnetic particles [57], as the latter may act as internal field enhancers amplifying the radical pair effect.

Finally, although measured at the products, the MFE by design is developed at the stage of the radical pair, and currently it is as direct as these difficult radicals can be sensed in solution. All attempts to directly observe paramagnetic NO and O_2^- in liquids by such standard magnetoresonance techniques as ESR invariably fail due to the features of their electronic structure, so instead elaborate indirect methods

developed for in vivo ESR have been used [58–61]. The MFE methodology, creating the radicals as a pair and monitoring the product of their recombination while applying magnetic field [62], is in this case a useful alternative to directly access the radicals, not the products of their chemical reactions. Building upon the well-understood behavior of radical pairs in solution, the suggested experiment can provide the missing link between the thoroughly studied properties of these simple molecules in the gas phase [63] and the studies at the physiological level which remain difficult to interpret [64–66]. The experiment can be further optimized by moving to higher magnetic fields and/or by restricting the orientational mobility of the molecules that presumably causes fast relaxation, e.g., by putting the system in a protein pocket or increasing the local viscosity. Similar effects in biological systems should be sought in the environments where biogenic iron is accumulated. Given the availability of high-field static magnets due to recent developments in NMR, it may be possible to measure the actual dependence of the reported MFE on magnetic field strength in the fields of up to 20 T (900 MHz NMR spectrometers) [67], and from this, estimate the mobility of NO in different environments and magnetic parameters of the free nitric oxide in liquid, including the magnitude of its spin–orbit coupling constant. It should be kept in mind, though, that this system is rather sensitive to such experimental conditions as temperature, pH, light, etc., and, if these are substantially changed, preliminary study of the system would be required. It is also critical to perform comparison against identical control samples kept in as identical conditions as possible, except for applying the magnetic field.

Acknowledgments We thank our colleagues from the Institute of Chemical Kinetics and Combustion SB RAS, Novosibirsk, Russia, M. Taraban and E. Glebov for critical discussions, I. Slepneva, D. Komarov and A. Bobko for help with sample preparation and optical measurements, I. Magin for help with high-field experiments and temperature check, E. Pritchina for help with statistics, and Dr. I. Kirilyuk from the Institute of Organic Chemistry SB RAS, Novosibirsk, Russia for the gift of the CpH spin trap. The work was supported by the International Association for the promotion of co-operation with scientists from the New Independent States of the former Soviet Union (INTAS), project 05-1000008-80, and by the Program "Leading Scientific Schools", Project 1875.2008.3.

References

1. A.K.A. Silva, E.L. Silva, E.S.T. Egito, A.S. Carrico, Radiat. Environ. Biophys. **45**, 245–252 (2006)
2. E. van Rongen, R.D. Saunders, E.T. van Deventer, M.H. Repacholi, Health Phys. **92**, 584–590 (2007)
3. H. Okano, Front. Biosci. **13**, 6106–6125 (2008)
4. U.E. Steiner, T. Ulrich, Chem. Rev. **89**, 51–147 (1989)
5. T.T. Harkins, C.B. Grissom, Science **263**, 958–960 (1994)
6. A.R. Jones, S. Hay, J.R. Woodward, N.S. Scrutton, J. Am. Chem. Soc. **129**, 15718–15727 (2007)
7. M.B. Taraban, T.V. Leshina, M.A. Anderson, C.B. Grissom, J. Am. Chem. Soc. **119**, 5768–5769 (1997)
8. A.C. Moller, L.F. Olsen, J. Am. Chem. Soc. **121**, 6351–6354 (1999)
9. A.R. Jones, N.S. Scrutton, J.R. Woodward, J. Am. Chem. Soc. **128**, 8408–8409 (2006)
10. M.S. Afanasyeva, M.B. Taraban, P.A. Purtov, T.V. Leshina, C.B. Grissom, J. Am. Chem. Soc. **128**, 8651–8658 (2006)
11. Y. Liu, R. Edge, K. Henbest, C.R. Timmel, P.J. Hore, P. Gast, Chem. Commun. **2**, 174–176 (2005)
12. A.L. Buchachenko, N.N. Lukzen, J.B. Pedersen, Chem. Phys. Lett. **434**, 139–143 (2007)
13. A.L. Buchachenko, D.A. Kouznetsov, N.N. Breslavskaya, M.A. Orlova, J. Phys. Chem. B **112**, 2548–2556 (2008)

14. W. Wiltschko, R. Wiltschko, Science **176**, 62–64 (1972)
15. T. Ritz, S. Adem, K. Schulten, Biophys. J. **78**, 707–718 (2000)
16. T. Ritz, P. Thalau, J.B. Phillips, R. Wiltschko, W. Wiltschko, Nature **429**, 177–180 (2004)
17. O. Efimova, P.J. Hore, Biophys. J. **94**, 1565–1574 (2008)
18. K. Maeda, K.B. Henbest, F. Cintolesi, I. Kuprov, C.T. Rodgers, P.A. Liddell, D. Gust, C.R. Timmel, P.J. Hore, Nature **453**, 387–390 (2008)
19. Y. Takashima, J. Miyakoshi, M. Ikehata, M. Iwasaka, S. Ueno, T.J. Koana, Radiat. Res. **45**, 393–397 (2004)
20. S. Nagakura, H. Hayashi, T. Azumi, *Dynamic Spin Chemistry* (Kodansha-Wiley, Tokyo, New York, 1998)
21. M.M. Triebel, A.K. Morozov, M.M. Totrov, G.E. Zorinyants, E.L. Frankevich, Chem. Phys. Lett. **214**, 321–326 (1993)
22. J.R. Woodward, T.J. Foster, A.T. Salaoru, C.B. Vink, Phys. Chem. Chem. Phys. **10**, 4020–4026 (2008)
23. R.J. Singh, N. Hogg, J. Joseph, E. Konorev, B. Kalyanaraman, Arch. Biochem. Biophys. **361**, 331–339 (1999)
24. M. Trujillo, M. Naviliat, M.N. Alvarez, G. Peluffo, R. Radi, Analusis **28**, 518–527 (2000)
25. C. Szabo, H. Ischiropoulos, R. Radi, Nat. Rev. Drug Discov. **6**, 662–680 (2007)
26. S. Goldstein, J. Lind, G. Merenyi, Chem. Rev. **105**, 2457–2470 (2005)
27. M. Feelisch, Naunyn–Schmiedeberg's Arch. Pharmacol. **358**, 113–122 (1998)
28. A. Schrammel, S. Pfeiffer, K. Schmidt, D. Koesling, B. Mayer, Mol. Pharmacol. **54**, 207–212 (1998)
29. S.V. Sergeeva, I.A. Slepneva, V.V. Khramtsov, Free Rad. Res. **35**, 491–497 (2001)
30. J.P. Crow, J.S. Beckman, J.M. McCord, Biochemistry **34**, 3544–3552 (1995)
31. A. Gomes, E. Fernandes, J.L.F.C. Lima, J. Fluoresc. **16**, 119–139 (2006)
32. J.P. Crow, Nitric Oxide Biol. Chem. **1**, 145–157 (1997)
33. L.M. Henderson, J.B. Chappell, Eur. J. Biochem. **217**, 973–980 (1993)
34. T. Ullrich, S. Oberle, A. Abate, H. Schroder, FEBS Lett. **406**, 66–68 (1997)
35. C.L. Fattman, L.M. Schaefer, T.D. Oury, Free Radical Biol. Med. **35**, 236–256 (2003)
36. K.M. Salikhov, Y.N. Molin, R.Z. Sagdeev, A.L. Buchachenko, *Spin Polarization and Magnetic Field Effects in Radical Reactions* (Elsevier, Amsterdam, 1984)
37. P.W. Atkins, M.C.R. Symons, *The Structure of Inorganic Radicals. An Application of Electron Spin Resonance to the Study of Molecular Structure* (Elsevier, New York, 1967)
38. E.V. Gorelik, N.N. Lukzen, R.Z. Sagdeev, U.E. Steiner, Chem. Phys. **262**, 303–323 (2000)
39. R. Beringer, J. G. Castle Jr., Phys. Rev. **78**, 581–586 (1950)
40. R.L. Brown, H.E. Radford, Phys. Rev. **147**, 6–12 (1966)
41. P.D.C. Dietzel, R.K. Kremer, M. Jansen, J. Am. Chem. Soc. **126**, 4689–4696 (2004)
42. H.C. Box, E.E. Budzinsky, K.T. Lilga, H.C. Freund, J. Chem. Phys. **53**, 1059–1065 (1970)
43. D.T. Sawyer, J.S. Valentine, Acc. Chem. Res. **14**, 393–400 (1981)
44. A.H. Cooke, H.J. Duffus, Proc. Phys. Soc. A **67**, 525–527 (1954)
45. P. Gilch, M. Linsenmann, W. Haas, U.E. Steiner, Chem. Phys. Lett. **254**, 384–390 (1996)
46. S. Dikalov, M. Skatchkov, E. Bassenge, Biochem. Biophys. Res. Comm. **231**, 701–704 (1997)
47. K. Doerffel, *Statistik in der Analitischen Chemie* (Grundstoffindustrie, Leipzig, 1966)
48. J. Garthwaite, Eur. J. Neurosci. **27**, 2783–2802 (2008)
49. S. Odenbach, J. Phys. Condens. Matter. **16**, R1135–R1150 (2004)
50. C. Holm, J.J. Weis, Curr. Opin. Colloid Interface Sci. **10**, 133–140 (2005)
51. N.G. Chalkias, P. Kahawong, E.P. Giannelis, J. Am. Chem. Soc. **130**, 2910–2911 (2008)
52. A. Kolnagou, Y. Michaelides, C. Kontos, K. Kyriacou, G.J. Kontoghiorghes, Hemoglobin **32**, 17–28 (2008)
53. I.B. Afanas'ev, Curr. Med. Chem. **12**, 2731–2739 (2005)
54. A.E. Oakley, J.F. Collingwood, J. Dobson, G. Love, H.R. Perrott, J.A. Edwardson, M. Elstner, C.M. Morris, Neurology **68**, 1820–1825 (2007)
55. Q. Pankhurst, D. Hautot, N. Khan, J. Dobson, J. Alzheim. Dis. **13**, 49–52 (2008)
56. K.L. Double, V.N. Dedov, H. Fedorow, E. Kettle, G.M. Halliday, B. Garner, U.T. Brunk, Cell. Mol. Life Sci. **65**, 1669–1682 (2008)
57. S. Johnsen, K.J. Lohmann, Nat. Rev. Neurosci. **6**, 703–712 (2005)
58. H.M. Swartz, N. Khan, V.V. Khramtsov, Antioxid. Redox Signal. **9**, 1757–1771 (2007)
59. F.A. Villamena, J.L. Zweier, Antioxid. Redox Signal. **6**, 619–629 (2004)
60. T. Nagano, T. Yoshimura, Chem. Rev. **102**, 1235–1269 (2002)

61. J. Vasquez-Vivar, P. Martasek, N. Hogg, H. Karoui, B.S.S. Masters, K.A. Pritchard, B. Kalyanaraman, Nitric Oxide, Pt. C, Methods Enzymol. **301**, 169–177 (1999)
62. E.V. Kalneus, D.V. Stass, Y.N. Molin, Appl. Magn. Reson. **28**, 213–229 (2005)
63. H. Ganser, W. Urban, A.M. Brown, Mol. Phys. **101**, 545–550 (2003)
64. P.D. Whissell, M.A. Persinger, Int. J. Dev. Neurosci. **25**, 433–439 (2007)
65. O. Sirmatel, C. Sert, C. Tumer, A. Ozturk, M. Bilgin, Z. Ziylan, Bioelectromagnetics **28**, 152–154 (2007)
66. J.C. Mckay, F.S. Prato, A.W. Thomas, Bioelectromagnetics **28**, 81–98 (2007)
67. B. Brocklehurst, Chem. Soc. Rev. **31**, 301–311 (2002)